

Adaptive Image Servo Controller for Robot-assisted Diagnostic Ultrasound

P. Abolmaesumi, M.R. Sirouspour, S.E. Salcudean, W.H. Zhu

The University of British Columbia
Department of Electrical and Computer Engineering
Vancouver, B.C., Canada, V6T 1Z4
puranga@ece.ubc.ca, tims@ece.ubc.ca

Abstract

A robot-assisted system for medical diagnostic ultrasound has been developed by the authors. An ultrasound image servo controller has already been proposed and implemented in [1, 2] to automatically compensate, through robot motions, unwanted motions in the plane of the ultrasound beam. This paper presents an adaptive image servo controller to enhance the performance of the ultrasound image servo controller. To increase safety, the control is shared between the operator and the image controller. The stability and accuracy of the system is illustrated through different experiments.

1 Introduction

Medical ultrasound exams often require that ultrasound technicians hold the transducers in awkward positions for prolonged periods of time, sometimes exerting large forces. A number of studies indicate that they suffer from an unusually high incidence of musculoskeletal disorders (e.g. [18]). Motivated initially by the need to alleviate these problems and to present a more ergonomic interface to the ultrasound technicians, a teleoperation approach to diagnostic ultrasound has been proposed. The system consists of a master hand controller, a slave manipulator that carries the ultrasound probe, and a computer control system that allows the operator to remotely position the ultrasound transducer relative to the patient's body. An inherently safe, light, backdrivable, counterbalanced robot has been designed and tested for use in carotid artery examinations, the purpose of which is to diagnose occlusive disease in the left and right common carotid arteries – a major cause of strokes [17].

The motion of the robot arm is controlled based on measured positions and forces, acquired ultrasound images, and/or taught position and force trajectories. The system uses a shared control approach that is ca-

pable of achieving motion, force and image control simultaneously.

The ability to interactively position the ultrasound probe via a teleoperated system, while being assisted with force and image controllers, has major advantages over other similar interfaces for ultrasound examination. In [13], a Mitsubishi PA-10 industrial robot was used with a force controller to assist ultrasound technicians to move the ultrasound probe against the patient's body. The ultrasound probe can only be moved by the robot, through a prespecified trajectory, which limits the flexibility of the examination. No shared control, teleoperation or ultrasound image servoing was reported. Other approaches, such as [4, 9], focus primarily on providing an interface for 3D ultrasound image reconstruction.

Automatically guiding the ultrasound probe as a function of its acquired images, an approach termed "ultrasound image servoing", could be a useful feature for diagnostic examinations when used in conjunction with human supervisory control, in order to reduce operator fatigue [1]. During the ultrasound examination, the operator interacts with a graphical user interface and a hand controller. The resulting operator commands are coordinated with the visual servo controller in order to control the robot, and thus the ultrasound-probe motion.

Adaptive visual servoing has already been proposed in the literature [3, 11, 12, 7, 10]. Papanikolopoulos [10] presents an adaptive control scheme for the problem of robotic visual servoing (eye-in-hand configuration) around a static rigid target. Hosoda [7] presents an adaptive visual servoing/force controller to realize visual servoing while the manipulator exerts contact force on a surface. The system only needs *a priori* knowledge of the manipulator. An estimator of the image Jacobian is presented to deal with the unknown environment. Asada [3] describes an adaptive binocu-

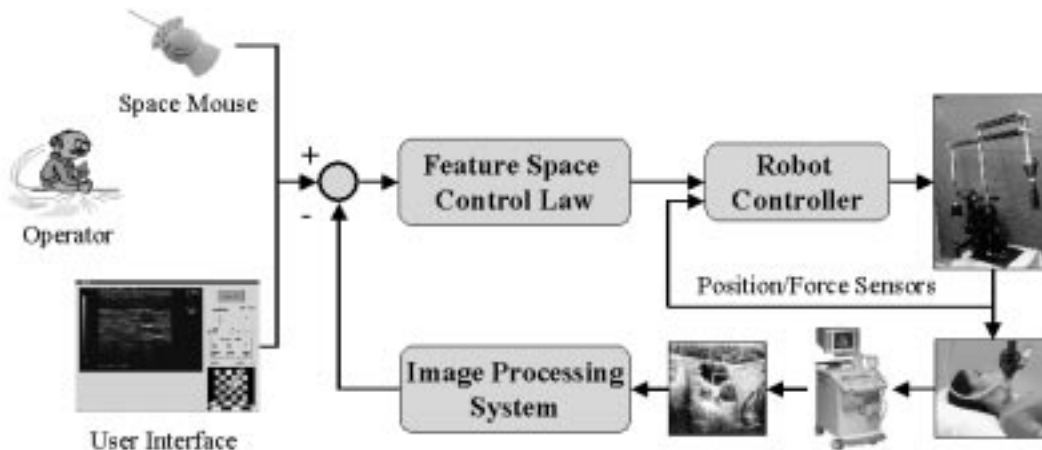


Figure 1: Block diagram of the ultrasound robot system.

lar visual servoing system to accomplish a given task in a dynamic environment. Piepmeier [11, 12] presents a dynamic quasi-Newton method to track a target by an uncalibrated model independent visual servo controller. The control problem is formulated as a non-linear least square optimization. A dynamic Jacobian estimation scheme is used to estimate the combined robot and image Jacobians. Experimental results are presented for a two-degree-of-freedom system.

This paper presents a new adaptive ultrasound image servo controller. Section 2 describes the system setup. Section 3 presents the theory behind ultrasound image servoing, along with the experimental results. The derivation of ultrasound image Jacobian estimator is presented in Section 4. Experiments are performed to compare the performance of the adaptive ultrasound image servo controller with the conventional controller. Finally, Section 5 provides a summary and concluding remarks.

2 System Setup

Figure 1 shows the block-diagram of the experimental setup. The system consists of a user interface, a slave manipulator carrying the ultrasound probe, and a computer control system.

2.1 The User Interface

The operator interacts with the system through the user interface, which consists of a master hand controller (a Space Mouse/Logitech Magellan [6]) and a graphical user interface (GUI). The velocity of all axes of the robot can be controlled by the Magellan mouse. The GUI allows the operator to activate/deactivate the robot, to enable/disable the force control and the

visual servoing and to enable/disable different degrees of freedom of the robot.

Ultrasound images are captured in real-time and are displayed in the GUI. For the ease of the operator, a 3D rendered model of the ultrasound probe, which displays the orientation of the transducer in real-time, is incorporated within the GUI. One or two features can be selected from the ultrasound image by using the mouse pointer. These features are passed to the image controller to compensate for motions in the plane of the ultrasound beam, the goal of which is to maintain features at the desired position in the image.

2.2 Ultrasound Robot

A lightweight robot with limited force capability has been designed for teleoperated ultrasound examinations [15]. The robot moves fast enough to allow ultrasound examination to take place at a pace close to that achieved by the unassisted sonographer. In addition, the robot joints are backdrivable so that the arm can be pushed out of the way if necessary and controlled effectively in force mode. During the ultrasound examination, the ultrasound transducer is carried by the end-effector of the robot. Small motor driving torques are required to generate a maximum force of 10 N at the end-effector, due to the fully counterbalanced mechanical design. This results in a system that is safe in the case of a power failure.

2.3 Robot Controller

The control approach is explained in [19]. Its objective is to let a linear combination of the velocity and scaled force of the ultrasound probe track the hand controller command (displacement). There is no explicit switching between the contact and free

motion states. The safety is insured by including a control “command reset” or “disturbance accommodation” function that never allows position errors to be large. The controller uses the measured probe positions and forces, the acquired ultrasound images, and/or the commanded position and force trajectories simultaneously in a shared control approach to control the robot arm.

3 Ultrasound Image Servoing

One of the main features of the current system is its ability to visually track features in ultrasound images in real-time. This could help ultrasound technicians in guiding the motion of the ultrasound probe during the examination. The image processing system captures the ultrasound images at a rate of 30 frames/s by using a Matrix VisionTM Mv-delta frame grabber. Ultrasound image servoing has been demonstrated by using the Star-Kalman motion tracking algorithm for a single degree of freedom [1, 2]. The feature tracking algorithm provides the image controller with the required feature coordinates (e.g. the center of the carotid artery) to control the robot. The feasibility of the ultrasound image servoing to control three axes of the robot can be determined by examining the ultrasound image Jacobian, which relates differential changes in the image features to differential changes in the configuration of the robot. Figure 2 illustrates the concept. Let $P_i = [u_i, v_i]^T$ be a feature point in the plane of the ultrasound image with coordinates $[e^x, e^y, e^z]^T$ in the probe-attached frame. Assuming an orthographic projection model [8] with scale a for the ultrasound image and that P_i remains in the image plane, the coordinates of P_i in the two-dimensional ultrasound image become $[u_i - u_0, 0, v_i]^T = [a^e x, 0, a^e z]^T$, where $[u_0, v_0]^T$ is the center of the ultrasound image. It can be shown that

$$\begin{bmatrix} \dot{u}_i \\ \dot{v}_i \end{bmatrix} = \begin{bmatrix} a & 0 & 0 & 0 & -v_i & 0 \\ 0 & 0 & a & 0 & u_i - u_0 & 0 \end{bmatrix} e\dot{X} = J_{v_i} e\dot{X} \quad (1)$$

where $e\dot{X}$ are the translational and angular end-effector velocities in end-effector coordinates and $J_{v_i} \in \mathbb{R}^{2n \times 6}$ is the ultrasound image Jacobian matrix. If several points are considered in the image, similar pairs of rows will be added to (1). The rank of the resulting Jacobian is at most three. Two or more feature points with motions not along the lines connecting them to each other will generate a Jacobian of rank three. Thus, as expected, with non-trivial ultrasound images, it is possible to control the motion of the ultrasound transducer in its image plane in three degrees of freedom.

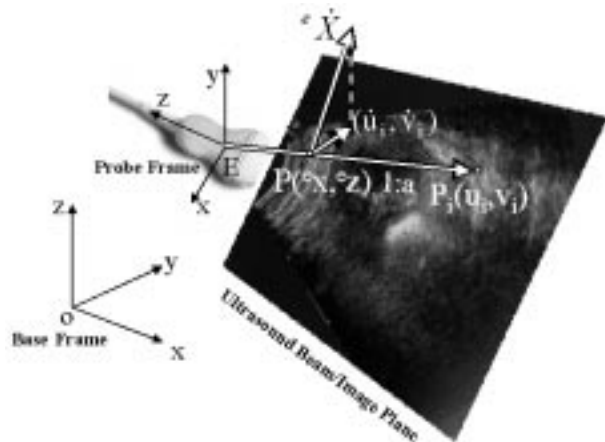


Figure 2: Definition of the frames for the ultrasound robot.

The visual controller, depicted in Figure 3, is described by:

$$e\dot{X} = -J_{v_i}^\dagger [K_d (f_i - f_r) - \dot{f}_r], \quad (2)$$

where $f_i = [u_i, v_i]^T$ is the actual image feature location in the ultrasound image, f_r is its desired location, K_d is the controller gain and $J_{v_i}^\dagger$ is the pseudo-inverse of J_{v_i} . $J_{v_i}^\dagger$ is the minimum norm solution of (1) to track one feature and the least square solution to track two or more features. Replacing J_{v_i} from (1) in (2) and assuming that the dynamics of the robot control loop are negligible relative to the image control loop, the following equation is derived:

$$\dot{f}_i + K_d f_i = K_d f_r + \dot{f}_r, \quad (3)$$

which guarantees that image feature servoing

$$(f_i) \longrightarrow (f_r) \quad (4)$$

can be achieved.

An ultrasound phantom has been designed to test the performance of the ultrasound image controller. Figure 4 illustrates a CAD model of the phantom. Three plastic tubes are positioned in a solution [14] along three different axes in the phantom.

Ultrasound image servoing at rates as high as 30 Hz has been achieved to control three axes of the robot, while tracking one or two features in the ultrasound image in real-time. With the coordinate system illustrated in Figure 2, the control axes are the translations along the x -axis and z -axis, while the rotation is about the y -axis. Figure 5 shows the ultrasound image servoing performance for one of the axes. For this

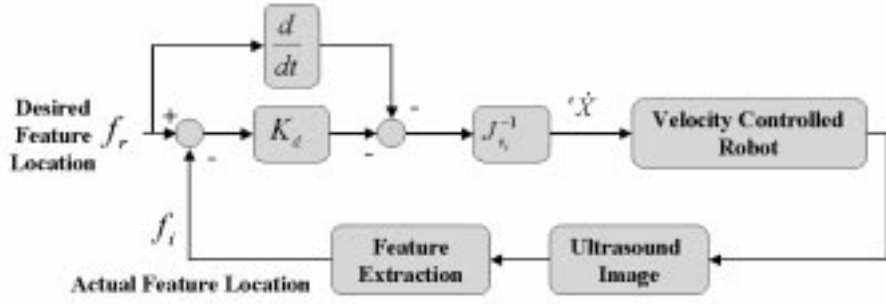


Figure 3: Ultrasound image controller.

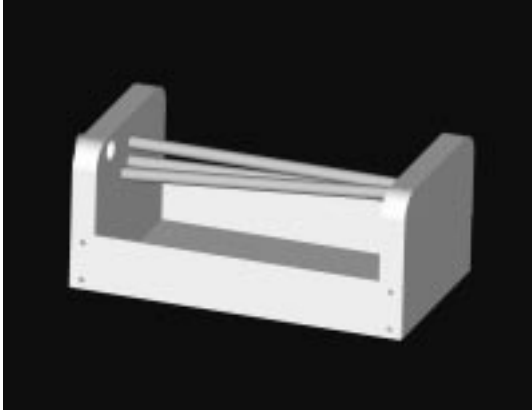


Figure 4: A CAD model of the ultrasound phantom.

experiment, a feature (center of one of the pipes in the phantom ultrasound image) is selected before enabling the visual servoing. While the operator is moving the probe along the y axis, the feature position is maintained in the center of the image automatically. The Star-Kalman algorithm [2] is used to extract the feature from the ultrasound image.

4 Adaptive Ultrasound Image Servoing

The performance of the ultrasound image servoing directly relates to the accuracy of the ultrasound image Jacobian. In the previous section, it was assumed that a model of the ultrasound image projection is known. This assumption may not be valid anymore when the operator changes the image parameters such as the magnification of the ultrasound image. In order to compensate for these changes in the image, a quasi-Newton adaptive method is proposed to update the ultrasound image Jacobian. By adopting an approach similar to [11], the following residual error can

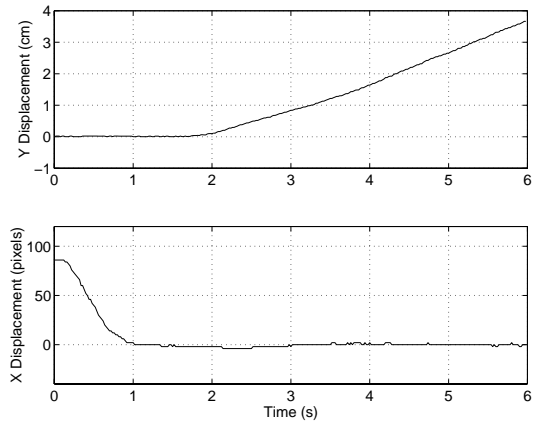


Figure 5: Experimental result for image servoing in single axis.

be defined:

$$\phi({}^e X, t) = f_i({}^e X) - f_r(t) \quad (5)$$

where ${}^e X$ is a vector of end effector coordinates in the end effector frame, $f_i({}^e X)$ is the position of the feature in the ultrasound image and $f_r(t)$ is the target position which is a function of time. The objective function, Φ , can be written as follows:

$$\Phi({}^e X, t) = \frac{1}{2} \phi^T({}^e X, t) \phi({}^e X, t) \quad (6)$$

Minimizing $\Phi({}^e X, t)$ with respect to ${}^e X$ for a fixed sampling rate Δt , the following visual controller can be proposed:

$${}^e \dot{X} = -\hat{J}_k^\dagger [K_d (f_i({}^e X_k) - f_r(t_k)) - \dot{f}_r(t_k)], \quad (7)$$

where ${}^e X_k$ is ${}^e X|_{t=t_k}$, \hat{J}_k^\dagger is the pseudo-inverse of \hat{J}_k and

$$\hat{J}_k = \left. \frac{\partial \phi}{\partial {}^e X} \right|_{{}^e X_k, t_k} \quad (8)$$

represents the k th approximation to the ultrasound image Jacobian. The convergence of the visual controller is discussed in [11, 12].

It can be shown that the following dynamic Broyden update provides a secant approximation to changes in the image Jacobian based on changes in the error function corresponding to changes in the state variables [11]:

$$\Delta \hat{J}_k = \frac{(\Delta \phi_k - \hat{J}_{k-1} \Delta^e X_k + \frac{df_r(t_k)}{dt} \Delta t_k) \Delta^e X_k^T}{\Delta^e X_k^T \Delta^e X_k} \quad (9)$$

where $\Delta \hat{J}_k = \hat{J}_k - \hat{J}_{k-1}$, $\Delta \phi_k = \phi(e X_k, t_k) - \phi(e X_{k-1}, t_{k-1})$ and $\Delta t_k = t_k - t_{k-1}$. Approximating

$$\frac{df_r(t_k)}{dt} = \frac{f_r(t_k) - f_r(t_{k-1})}{t_k - t_{k-1}} \quad (10)$$

and dividing the numerator and denominator of (9) by Δt_k^2 , we get to the following simplified formula:

$$\Delta \hat{J}_k = \frac{(\dot{f}_i(X_k) - \hat{J}_{k-1} \dot{X}_k) e \dot{X}_k}{e \dot{X}_k^T e \dot{X}_k} \quad (11)$$

The result shows that for the first order approximation, the change in \hat{J}_k is not related to the target motion in time.

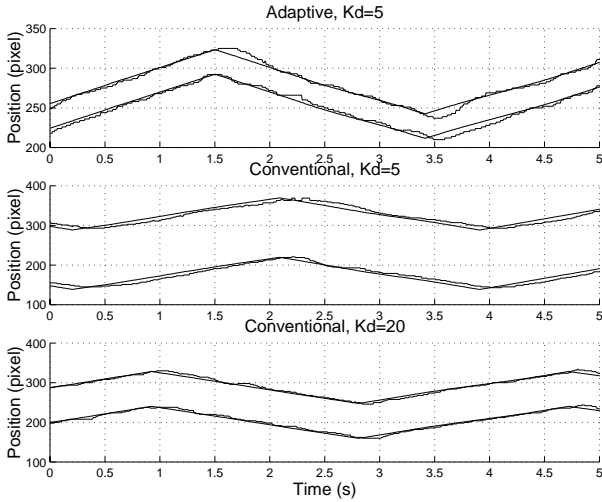


Figure 6: Experimental results for adaptive and conventional ultrasound image servo controllers. $K_d = 5$ for the adaptive controller and $K_d = 5$ and $K_d = 20$ for the conventional controller. In each figure, the tracking results for x -axis (top) and z -axis (bottom) are displayed.

Experiments show a satisfactory performance of the adaptive ultrasound image servoing method. In all of

the experiments, a feature is tracking a simulated target which moves in the image along a line with equation $v = -(u - u_{i0}) + v_{i0}$, where $[u_{i0}, v_{i0}]^T$ is the initial coordinates of the feature. A sequential similarity detection algorithm [5] is used to track the feature in the ultrasound image. Figure 6 compares the performance of the adaptive and conventional ultrasound image servo controllers. The initial condition for the adaptive ultrasound image Jacobian estimator, \hat{J}_0 , is chosen equal to J_{v_i} . \hat{J}_k converges after 5 s. The standard deviation of errors are $\sigma_x = 3.88$ and $\sigma_y = 4.35$ for the adaptive method and $\sigma_x = 7.52$ and $\sigma_y = 6.28$ for the conventional method. However, the performance of the conventional method can be improved by increasing the controller gain. Figure 6 demon-

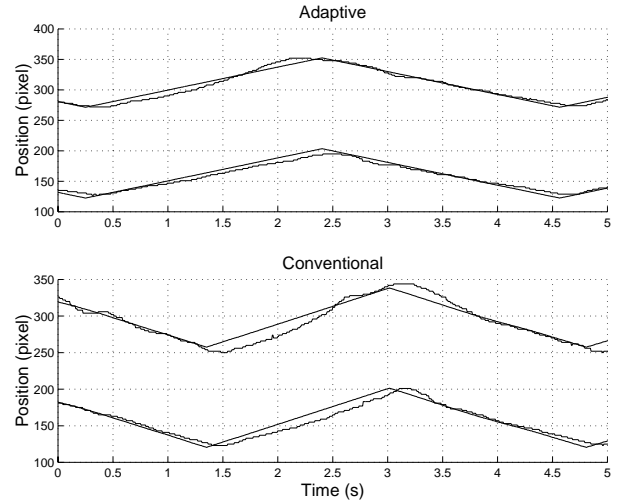


Figure 7: Experimental results for adaptive and conventional ultrasound image servo controllers with $K_d = 5$ and $K_d = 20$, respectively. Ultrasound images are scaled down to 65% of their original size. In each figure, the tracking results for x -axis (top) and z -axis (bottom) are displayed.

strates the performance of the conventional method with $K_d = 20$. The standard deviation of errors are $\sigma_x = 3.93$ and $\sigma_y = 3.74$ which show similar performance to that of the adaptive controller. In order to see the effect of the accuracy of the image projection model on the performance of the ultrasound image servo controllers, ultrasound images were scaled down to 65% of their original size. Figure 7 compares the performance of the two controllers. The standard deviation of errors are $\sigma_x = 4.65$ and $\sigma_y = 4.42$ for the adaptive method and $\sigma_x = 9.04$ and $\sigma_y = 6.17$ for the conventional method which show better performance by the adaptive ultrasound image servo controller.

5 Summary and Conclusions

A new medical ultrasound examination system that uses a robot to remotely position the ultrasound probe was presented. The system uses a shared control approach that is capable of achieving motion, force and image control simultaneously. An ultrasound image servoing capability is embedded in the system. An adaptive ultrasound image servo controller is proposed and the performance is compared with the conventional controller. The results show similar performance of both approaches when the image projection model is accurate, but better performance of the adaptive controller when the image parameters are changed.

In the future, the passive mouse will be replaced by a PowerMouse haptic interface [16], in order to realize bilateral teleoperation with force feedback. Also, the system will be used and tested for ultrasound diagnostic at the Vancouver General Hospital, UBC. A human factors study to compare the presented approach with that of the conventional ultrasound examination is also under way.

References

- [1] P. Abolmaesumi, S.E. Salcudean, and W.H. Zhu. Visual servoing for robot-assisted diagnostic ultrasound. *World Congress on Medical Physics and Biomedical Engineering*, Chicago, 2000.
- [2] P. Abolmaesumi, M.R. Sirouspour, and S.E. Salcudean. Real-time extraction of carotid artery contours from ultrasound images. *Computer-Based Medical Systems*, pages 181–186, Texas, June 2000.
- [3] M. Asada, T. Tanaka, and K. Hosoda. Adaptive binocular visual servoing for independently moving target tracking. *Proc. ICRA*, San Francisco, CA, 2000.
- [4] K. Baba, K. Satch, S. Satamoto, T. Okai, and I. Shiego. Development of an ultrasonic system for three-dimensional reconstruction of the foetus. *J. Perinat. Med.*, 17, 1989.
- [5] L.G. Brown. A survey of image registration techniques. *ACM*, 1992.
- [6] J. Dietrich, G. Plank, and H. Kraus. Optoelectronic system housed in plastic sphere. Europ. Patent No. 0 240 023; US-Patent No. 4,785,180; JP-Patent No. 1 763 620.
- [7] K. Hosoda, K. Igarashi, and M. Asada. Adaptive hybrid visual servoing/force control in unknown environment. *Proc. IROS*, 1996.
- [8] S. Hutchinson, G. Hager, and P.I. Corke. A tutorial on visual servo control. *IEEE Trans. on Rob. Auto.*, 12(5):651–670, October 1996.
- [9] R. Ohbuchi, D. Chen, and H. Fuchs. Incremental volume reconstruction and rendering for 3-d ultrasound image. *Vis. Biomed. Comput.*, pages 312–323, 1992.
- [10] N.P. Papanikolopoulos and P.K. Kholsa. Adaptive control techniques for dynamic visual repositioning of hand-eye robotic systems. *IEEE*, 1992.
- [11] J.A. Piepmeier, G.V. McMurray, and H. Lipkin. A dynamic jacobian estimation method for uncalibrated visual servoing. *IEEE Int. Conf. Adaptive Intelligent Mechatronics*, 1999.
- [12] J.A. Piepmeier, G.V. McMurray, and H. Lipkin. A dynamic quasi-newton method for uncalibrated visual servoing. *Proc. ICRA*, 1999.
- [13] F. Pierrot, E. Domre, and E. Dgoulange. Hippocrate: A safe robot arm for medical applications with force feedback. *Medical Image Analysis*, 3:285–300, 1999.
- [14] D.W. Rickey, P.A. Picot, D.A. Christopher, and A. Fenster. A wall-less vessel phantom for doppler ultrasound studies. *Ultrasound in Medicine and Biology*, 21(9):1163–76, 1995.
- [15] S.E. Salcudean, G. Bell, S. Bachmann, W.H. Zhu, P. Abolmaesumi, and P.D. Lawrence. Robot-assisted diagnostic ultrasound - design and feasibility experiments. *MICCAI'99*, Cambridge, UK, September 1999.
- [16] S.E. Salcudean and N.R. Parker. 6-dof desk-top voice-coil joystick. *6th Symp. Haptic Inter. for Virtual Env. and Teleop. Sys., Intl. Mech. Eng. Congr. Exp.*, 61:131–138, November 16–21 Dallas, Texas, 1997.
- [17] S.E. Salcudean, W.H. Zhu, P. Abolmaesumi, S. Bachmann, and P.D. Lawrence. A robot system for medical ultrasound. *ISRR'99*, pages 152–159, Oct. 9–12 Snowbird, Utah, 1999.
- [18] H.E. Vanderpool, E.A. Friis, B.S. Smith, and K.L. Harms. Prevalence of carpal tunnel syndrome and other work-related musculoskeletal problems in cardiac sonographers. *Journal of Occupational Medicine*, 35:604–610, June 1993.
- [19] W.H. Zhu, S.E. Salcudean, S. Bachman, and P. Abolmaesumi. Motion/force/image control of a diagnostic ultrasound robot. *Proc. IEEE Int. Conf. Rob. Auto.*, San Francisco, 2000.